PNAS
www.pnas.org

Supplementary Information for

Building a synthetic mechanosensitive signaling pathway in compartmentalized artificial cells

James W. Hindley†, Daniela G. Zheleva†, Yuval Elani, Kalypso Charalambous, Laura M. C. Barter, Paula J. Booth, Charlotte L. Bevan, Robert V. Law and Oscar Ces

† These authors contributed equally.

Corresponding Author: Oscar Ces

Email: o.ces@imperial.ac.uk

This PDF file includes:

www.pnas.org/cgi/doi/10.1073/pnas.1903500116

Supplementary Materials and Methods

1,2-dioleoyl-sn-glycero-3-phophocholine (DOPC), 1,2-dioleoyl-sn-glycero-3-phophoglycerol (DOPG) and 1-palmitoyl-2-oleoyl-sn-glycero-3-phosphocholine (POPC) were obtained from Avanti Polar Lipids™ (USA). Detergent Octyl-β-D-Glucopyranoside (OG) was purchased from Affymetrix (USA). SM-2 Adsorbant BioBeads were purchased from BioRad (USA). All other reagents were purchased from Sigma Aldrich (UK).

Expression and purification of recombinant G22C F93W MscL

E. coli BL21 (DE3) cells carrying the pET28a (Novagen) vector with chemically gated MscL gene (G22C and F93W mutations) were grown overnight in Luria broth (LB) (30μg/ml kanamycin) at 37°C and 250 rpm. The overnight culture was then reseeded 1:100 into 1L fresh LB (30μg/ml kanamycin) and incubated at 37°C and 250 rpm to the maximum of the exponential phase (OD600 = 1). Note that all subsequent volumes are for expression and purification from 6L fresh LB. Protein production then induced for 90 min in the presence of isopropyl β-D-thiogalactopyranoside (IPTG) (0.5 mM). MscL was purified using a modified protocol of Perozo et al.(1). Briefly, cells were collected by centrifugation at 16,000g (45 minutes, 4°C) and resuspended in 50ml of 20mM HEPES, 100mM KCl and 0.1mM phenylmethanesulfonylfluoride (PMSF) solution. Cells were then lyzed by two passages through a cell disruptor (Constant Systems Cell Disruptor Model T5) at 25 kpsi. Membrane fractions were isolated through centrifugation (100,000g, 1hr, 4°C) and solubilised in solubilisation buffer (20 mM HEPES pH 7.2, 100 mM KCl, 2% (w/v) DDM, EDTA-free cOMPLETE protease inhibitor) overnight with rotation. Insoluble material removed by centrifugation (100,000g, 45 min, 4°C). Supernatant diluted 2-fold in 20 mM HEPES pH 7.2, 100 mM KCl and DDM-solubilised protein batch-bound to 4ml TALON cobalt metal affinity resin with rotation for 90 min at 4°C. Centrifugation at 1000g until resin pelleted (5-10 min) and supernatant removed, avoiding disturbing the pellet.

Non-specific protein binding was removed by washing the resin with 40 ml wash buffer (20 mM HEPES pH 7.2, 100 mM KCl, 0.13% DDM, 0.1mM PMSF and 6 mM imidazole), incubating the suspension for 10 min at 4°C with rotation. The resuspended resin was pelleted again via centrifugation (1000g, 5-10 min), supernatant removed and pellet resuspended in 10 ml wash buffer and transferred to a gravity-flow column where the resin was allowed to settle out of suspension. MscL was eluted in 15 ml elution buffer (20 mM HEPES pH 7.2, 100 mM KCl, 0.13% DDM, 0.1 mM PMSF, 150 mM imidazole) and concentrated to ~2 ml using an Amicon Ultra 100,000 MWCO centrifugal concentrator (Millipore). Imidazole removed using a PD-10 desalting column (GE Healthcare) and concentrated again using an Amicon Ultra 100,100 MWCO centrifugal concentrator before being snap frozen in liquid nitrogen and stored at -80°C until reconstitution. The concentration of purified MscL was then quantified using a NanoDrop 2000 UV-vis Spectrophotometer (Thermo Scientific), measuring the absorbance at 280 nm. Average MscL concentrations varied between 0.15- 1.5 mM of MscL pentamer.

Preparation of 1:1 DOPC:DOPG large unilamellar vesicles containing reconstituted MscL

To prepare 12.5 mM (5mg) of 1:1 DOPC:DOPG (mol/mol) lipid films, 2.5 mg of DOPC and 2.53 mg DOPG were weighed out and dissolved in chloroform. This lipid solution

was then gently mixed for 2 min before evaporating the chloroform under a stream of N_2(g) and storing the resultant film under vacuum overnight at room temperature. Films were rehydrated with 40 mM octyl-β-D-glucopyranoside (OG), 50 mM calcein, 20 mM HEPES, 100 mM KCl at pH 7.4 to a concentration of 10 mg/ml and freeze-thawed 3 times, flash-freezing the suspension in N_2(l) each time before heating to 50°C and vortexing for 1 minute at a time. Vesicles were extruded through 0.1 μm polycarbonate filters 11 times to produce a suspension of large unilamellar vesicles ~ 100 nm in diameter.

Vesicles were then added to G22C F93W MscL at a 50,000:1 lipid:protein molar ratio, and left on rotator bars for 45 minutes at 4°C. OG was then removed through the addition of 300 mg of SM-2 Bio-Beads (mesh size 25-50, Bio Rad (USA)) in 3 x 100 mg batches, leaving the lipid-MscL-OG suspension on rotator bars for 1 hour with each batch of beads at 4°C**.** Unencapsulated calcein was then removed by size-exclusion chromatography using a Sephadex G-50 column, eluting the sample with sucrose buffer (500 mM sucrose, 100 mM KCl, 20 mM HEPES, pH 7.4) in fractions of 300μl. Control samples (-MscL) were prepared identically except with the addition of 0.13 % DDM.

Formation of nested vesicles via emulsion phase transfer

2.63 mM (4 mg) POPC was suspended in mineral oil (2 ml), vortexed for 60 seconds and sonicated at 37 Hz for 45 minutes to give a lipid-in-oil solution. The aqueous phase was created by mixing calcein loaded MscL-vesicles 1:1 (v/v) with a phospholipase solution (1 nM b.v. $sPLA_2$, 5 mM EDTA, 500 mM sucrose, 20 mM HEPES, 100 mM KCl pH 7.4). The $sPLA_2$/EDTA solution was mixed with a pipette, then left to incubate for 10+ minutes before combination with vesicles to ensure inactivation of $sPLA_2$ due to calcium chelation.

Emulsions were then generated at 10:1 (v/v) of POPC in mineral oil: aqueous phase containing MscL-vesicles, $sPLA_2$ and EDTA in sucrose buffer by combining both phases and pipetting 5-10 times until a homogeneous emulsion was formed. The emulsion was then layered on top of a glucose buffer (500mM glucose, 20 mM HEPES, 100 mM KCl pH 7.4) before centrifuging the sample for 15 minutes at 9000 x g at room temperature to form a nested vesicle pellet. The oil and glucose was removed before re-suspending the nested vesicles in fresh glucose buffer, and any free calcein/MscL vesicles/$sPLA_2$ was removed by re-pelleting the vesicles through centrifugation for 10 minutes at 6000 x g, removing the glucose supernatant and re-suspending the nested vesicles again. This process was carried out twice before further experiments. For spectroscopy-based experiments, sucrose buffer was used for the final vesicle re-suspension to ensure that the vesicles did not settle due to density differences in the spectrometer well-plate.

Fluorescence Spectroscopy of Vesicles

The fluorescence of all vesicle samples was recorded in 96-well plates, with calcein fluorescence emission recorded at $\lambda_{ex/em}$ = 494/514 nm. Large unilamellar DOPC:DOPG vesicles +/-MscL were diluted in sucrose buffer at a 1:50 (v/v) ratio, whilst nested vesicles +/-MscL were diluted in sucrose buffer at a 1:8 (v/v) ratio. Baseline recordings

(F_0) were collected for 10+ minutes prior to reagent addition in all experiments. Triton X-100 (3 v/v%) was added at the end of each assay, left for 15 minutes to enable complete vesicle lysis and then the samples were imaged for a further 10 minutes (complete lysis was established by negligible change in fluorescence during final imaging, as well as upon the addition of further Triton X-100). Measurement of lysed vesicles provides the maximum fluorescence value for each well (F_{END}), allowing for normalization of results. Since the amount of vesicles in each well remains constant, the percentage and rate of fluorescence increase can be directly related to the release of dye through open MscL pores(2, 3). Normalized fluorescence data was obtained using equation (1), where F_t is the fluorescence value at time t.

$$Calcein\ Flux\ (\%) = \frac{F_t - F_0}{F_{END} - F_0} * 100 \qquad (1)$$

Triggering MscL opening using $sPLA_2$

$sPLA_2$ was added at concentrations ranging from 0.05 nM to 5 nM (final concentration) to wells containing LUVs +/-MscL. Sample fluorescence was recorded every 5 minutes for two hours before lysis.

Inactivating sPLA2 in LUV experiments

EDTA was added at concentrations from 0.25 mM to 2.5 mM (final concentration) to wells containing LUVs +/- MscL mixed and incubated for 1 hour. $sPLA_2$ (0.5 nM) was then added to each well and sample fluorescence was recorded every 2 minutes for a further hour.

Reactivating mechanosensitive networks through Ca^{2+} addition

EDTA (2.5 mM) was added to wells containing LUVs +/-MscL and incubated for 1 hour. $sPLA_2$ (0.5 nM) was added and the fluorescence was measured for 45 minutes to ensure network inactivation. $CaCl_2$ was then added at 0.25 mM – 10 mM (final concentration) before recording sample fluorescence every 5 minutes for a further 100 minutes.

Activating the mechanosensitive pathway in nested vesicles

αHL was added to nested vesicle-containing wells at a 1:10 ratio. After 45 minutes of imaging, $CaCl_2$ was added at 2.5 mM – 30 mM. The sample fluorescence was recorded every 10 minutes for a further 3 hours. When testing the stability of nested vesicles, samples were diluted in sucrose buffer at a 1:8 (v/v) ratio as above without adding $CaCl_2$, and sample fluorescence was recorded every 10 minutes for 15 hours.

Optical and Fluorescence Microscopy of Vesicles

GUVs were imaged on a Nikon Eclipse TE 2000-E Inverted Microscope connected to a QICAM camera (QImaging, Surrey, Canada) illuminated by a mercury arc lamp. The TRITC filter (Ex. 535 nm, Em. 590nm, dichroic 575 nm) and the FITC filter (Ex. 489 nm, Em. 535 nm, dichoric 505 nm) were used to capture rhodamine and calcein fluorescence respectively. Phase contrast and fluorescence images were taken of all samples. All images were analyzed and manipulated using ImageJ software (National

Institute of Health, USA). Fluorescence intensity was extracted using the Mean Grey Value option.

Samples were imaged on 1% BSA-coated glass imaging slides to prevent wetting and rupture of the nested vesicles to the glass surface. Slides produced by depositing a 50 µL of 1% BSA in DI on the glass slide, followed by evaporation of the solution overnight in a 60°C oven to leave a protein film. Slides then rinsed under a stream of DI water and dried with N_2(g) to leave behind a dry protein monolayer.

Nested vesicles were imaged in wells containing the following: 4:4:1:1 nested vesicles:glucose buffer:$CaCl_2$ (100mM; final concentration = 10 mM)) in glucose buffer, αHL (0.5 mg/ml; final concentration = 0.05 mg/ml in citrate buffer as provided by Sigma Aldrich). For control experiments without αHL an equal volume of glucose buffer was added, and for controls without MscL nested vesicles were created with 1:1 DOPC:DOPG vesicles lacking the channel. The solution was mixed to ensure αHL insertion into nested vesicle membranes. When monitoring activation of the mechanosensitive pathway in single vesicles, images were taken on a 20x magnification every two minutes in both bright-field and fluorescence (FITC) channels. A 100 ms exposure time was used for bright-field and 500 ms exposure time was used for fluorescence measurements. To minimise photobleaching the lamp was turned off immediately after each sample acquisition. Fluorescence was normalised with respect to vesicle volume and the fluorescence increase was recorded as a % increase from the vesicle fluorescence at t = 0 minutes.

Confocal Fluorescence Microscopy of Vesicles

A Leica TCS SP5 confocal fluorescent microscope was used with a 20× objective set with a 113.2 µm pinhole. The field of view was set to 775 × 775 µm (512 × 512 pixels) and the samples were acquired at a frequency of 400 Hz with one line average. The excitation was achieved with a wavelength of 543 nm (HeNe 543 laser) and absorbance was set at between 560 and 600 nm. DOPC:DOPG:Rhod-PE (50:49:1 molar ratio) LUVs were prepared at 10 mg/ml in sucrose buffer (0.5M sucrose, 20 mM HEPES, 100 mM KCl pH 7.4), freeze-thawed 4 times and extruded 11 times through a 100 nm filter before diluting to the relevant concentration. Slides and nested vesicles were prepared as above and nested vesicles diluted 2-fold in glucose buffer before imaging. Extracted grey scale fluorescence values were converted into a lipid concentration through use of a Rhod-PE-labelled PC:PG (1:1 molar ratio) LUV calibration curve (Appendix SI, Figure S5). Encapsulation efficiencies were then estimated using the equation (2):

$$Encapsulation\ Efficiency\ (\%) = \left(\frac{C_{encap}}{C_{initial}}\right) * 100 \qquad (2)$$

Where c_{encap} and $c_{initial}$ are the encapsulated and initial lipid concentration respectively.

Dynamic Light Scattering of Large Unilamellar Vesicles

DLS data was obtained on a Delsa™ Nano C Particle Analyser (Beckman Coulter, USA) with an argon ion laser light source using a 514.5 wavelength beam. Scattered light was detected at an angle of 163 °C from the transmitted beam to minimize

the effects of reflection. Vesicle samples run at 1 mg/ml concentration. 30 mM $CaCl_2$ was added when monitoring calcium induced size changes. The sample was gently pipetted each time to ensure complete suspension and imaged at 0, 60 and 180 minutes after $CaCl_2$ addition.

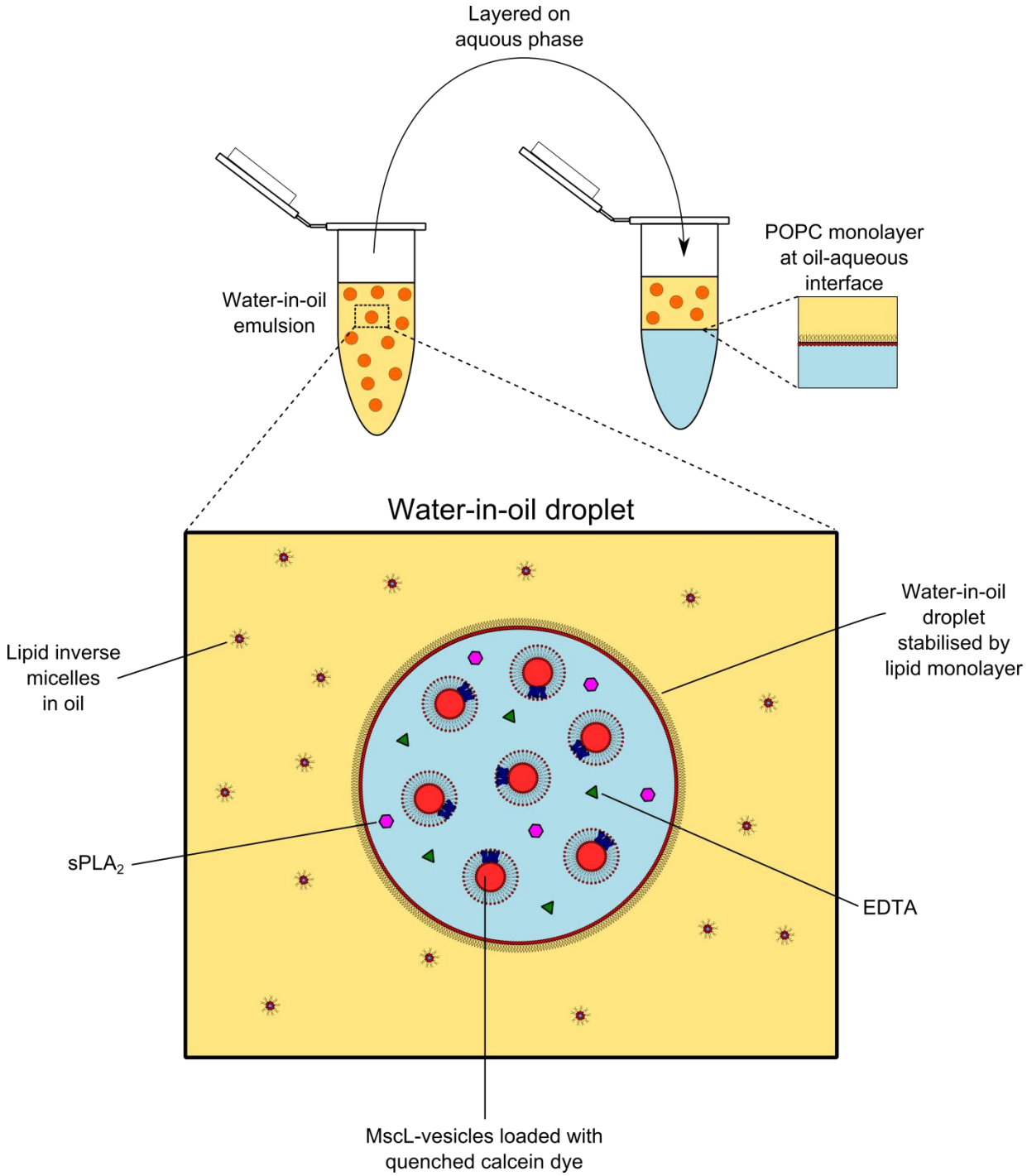

Fig. S1. Cartoon illustrating the emulsion phase-transfer process used to create nested vesicles. Emulsions are created by combining POPC (1-palmitoyl-2-oleoyl-glycero-3-phosphocholine) in mineral oil with an aqueous phase containing MscL-LUVs loaded with quenched (50 mM) calcein, sPLA2 and EDTA which chelates any residual calcium in the emulsion. By layering this emulsion on an aqueous layer, the POPC monolayer-stabilised droplets pick up a second monolayer as they cross the oil-water interface, forming giant nested vesicles (or vesosomes).

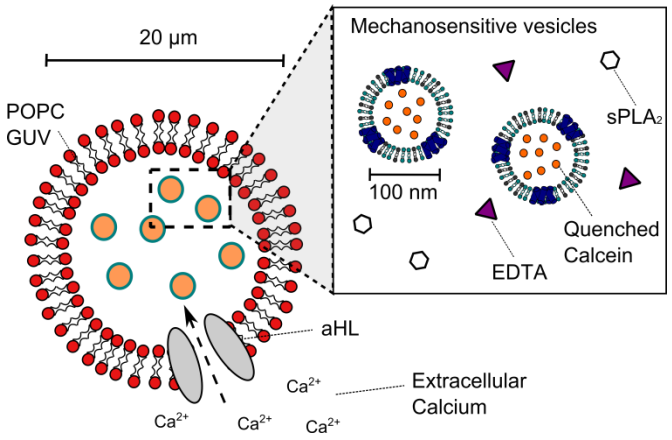

Fig. S2. Cartoon of fully-assembled artificial cell containing the mechanosensitive signaling pathway. See table S1 for notes on each component of the artificial cell.

Table S1. Composition of nested artificial cells containing the mechanosensitive signaling pathway.

Component	Concentration	Notes
GUV composition: POPC	2 mg/ml in initial oil solution	POPC is chosen in this work due to its mimicking of mammalian phospholipid composition. It also forms stable GUVs when using the phase transfer technique(4).
Mechaonsensitive vesicle composition: Calcein-loaded DOPC:DOPG Vesicles + MscL G22C F93W	3.1 mM (~2.5 mg/ml) lipid concentration in emulsion droplets	By making these vesicles highly negatively charged (~50 mol% DOPG which is anionic at experimental pH) they are stabilised through electrostatic repulsion. The high PG content also has been shown to result in high efficiencies of MscL channel activation(2). The G22C and F93W mutations in MscL enable chemical activation of the channel with methanethiosulfonate reagents(5) and quantification of the protein by UV-vis spectroscopy respectively.
$sPLA_2$ (bee venom)	0.5 nM (3 U/ml)	Bee venom $sPLA_2$ has been used in this study due to its successful implementation in previous work(3).
EDTA	2.5 mM	This concentration is established in this study to be sufficient for network inactivation, and hence was used in all nested vesicle experiments.
+αHL	0.05 mg/ml in external solution	αHL is a useful tool for membrane permeabilization due to its high water solubility and pore stability once formed.
$+Ca^{2+}$	10 mM in external solution for successful vesicle activation	Ca^{2+} at high concentrations can result in aggregation in PG-rich vesicles(6). This behaviour could be reduced in future work by reducing the PG content in the internal vesicles or adding PEGylated lipids to MscL-vesicles.

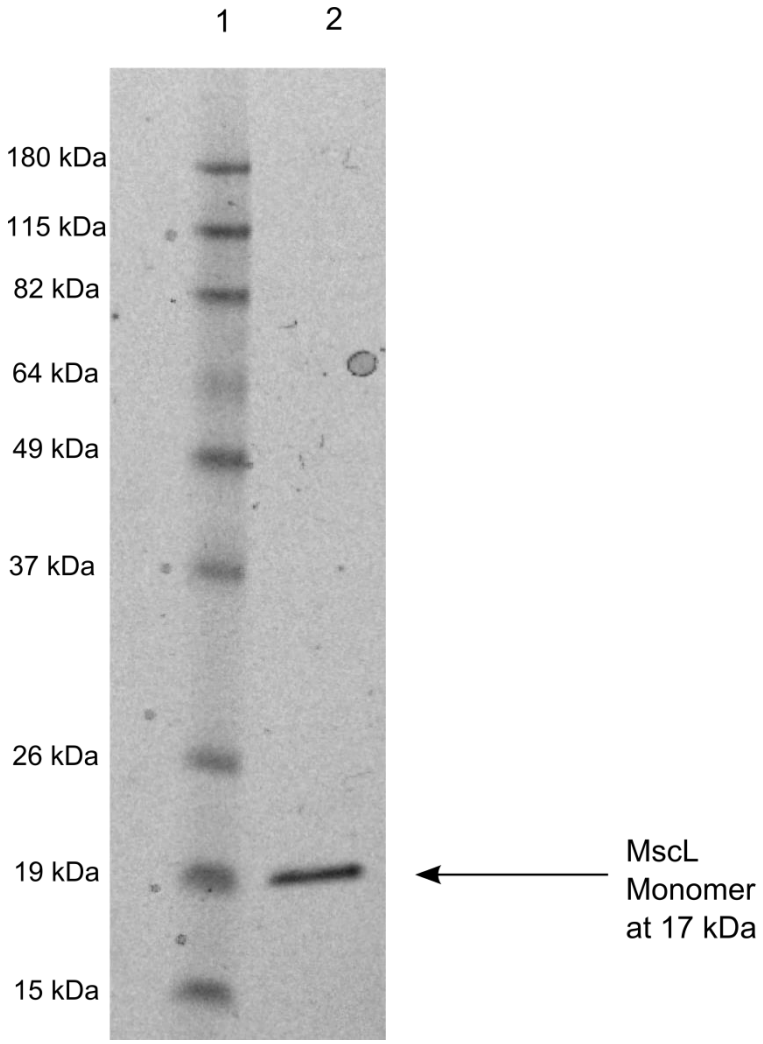

Fig. S3. SDS Gel-electrophoresis of purified recombinant G22C, F93W MscL. Gel electrophoresis containing 1. Novex Sharp Protein Standard Ladder and 2) MscL at 0.5 mg/ml. MscL is detected ~19 kDa, as expected due to its monomer molecular weight of ~17 kDa. The gel was run on pre-cast NuPAGE 12% Bis-Tris Proteins Gels using NuPAGE MOPS SDS Running Buffer and NuPAGE LDS Sample Buffer (Thermo Fisher Scientific, USA). Samples prepared as advised from manufacturer and the gel was run at 200V constant for 50 minutes before staining with InstantBlue (Expedeon) for 1 hour before washing the gel in DI water overnight. Imaging was performed using a Fuijfilm LAS-3000 (Fujifilm, Japan) and ImageQuant LAS 4000 software with 0.5s exposure time.

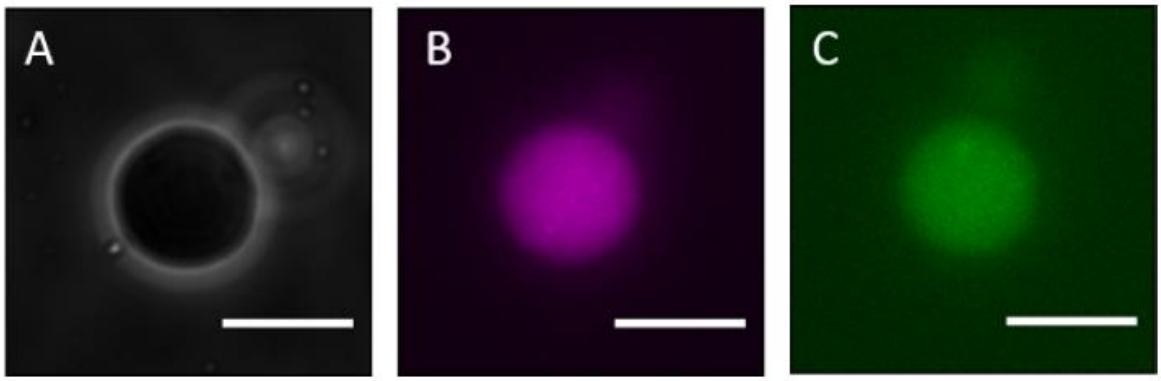

Fig. S4. Confirming successful encapsulation of the full system via optical and fluorescence microscopy. A. Phase contrast microscopy shows the characteristic 'halo' around the vesicle, indicating that a bilayer has successfully formed. **B.** By placing the fluorescent lipid Rhodamine-PE (1 mol%) in 1:1 DOPC:DOPG vesicles they can be visualized in the lumen of the giant vesicle. This fluorescence is localized to the giant vesicle indicating successful encapsulation of the nanoscale vesicles within the microcompartment. **C.** Calcein is encapsulated within the 1:1 DOPC:DOPG vesicles. The higher background fluorescence compared to B. indicates that some dye is present in external solution, attributed to insufficient purification of the nested vesicle through pelleting and removal of supernatant containing free calcein and LUVs. The higher fluorescence within the GUV confirms that the majority of the dye remains encapsulated. Scale bar for each image = 20 μm.

Supplementary Note 1. Quantifying the Encapsulation of DOPC:DOPG vesicles within POPC giant vesicle structures.

Although the experiments in SI Appendix Figure S4 confirmed successful nested vesicle formation, quantification of LUV encapsulation efficiency is essential to evaluate vesicle composition and enable analysis of encapsulated component functionality. To address this, confocal fluorescence microscopy was used to quantify the encapsulation of rhodamine PE-labelled LUVs in nested systems. The fine spatial resolution of confocal microscopy leads to reduced error in measurements compared to widefield microscopy, improving the accuracy of encapsulation efficiency estimation(7). The average encapsulation efficiency of PC:PG vesicles at millimolar concentration in POPC GUVs was estimated to be 67.59 ± 1.94 %, (SI Appendix, Table S2) as estimated using the linear relationship in PC:PG lipid concentration and Rhodamine-PE fluorescence obtained between 0.0225 – 6.35 mM (r^2 = 0.992, SI Appendix, Figure S5A). This loss is attributed to the rupture of encapsulated vesicles to stabilize the water/oil interface during emulsion generation. When lipids are present in both phases, competition occurs between vesicles rupturing from the aqueous phase and inverse micelles rupturing the oil phases during monolayer formation, leading to the disruption of a percentage of the encapsulated vesicle population(8). These efficiencies may therefore be increased above ~70% if greater lipid concentrations are encapsulated in the oil and/or water phases during emulsion generation.

It can therefore be assumed that successful production of a nested vesicle with millimolar internal lipid content occurs with ~30% loss of LUV content during the emulsion phase transfer process. This is acceptable for the proof-of-principle work undertaken here and compares favourably to previous studies of nested vesicle encapsulation efficiency. Previous hydration-based methods of nested vesicle (or vesosome) production have yielded encapsulation efficiency averages of ~50-60%(9–11), indicating that emulsion methods out-perform the production of nested vesicles through sequential extrusion(11) and perform at least equally as well as nested vesicles produced through the encapsulation of LUVs during cochleate cylinder to giant vesicle transition(9, 12).

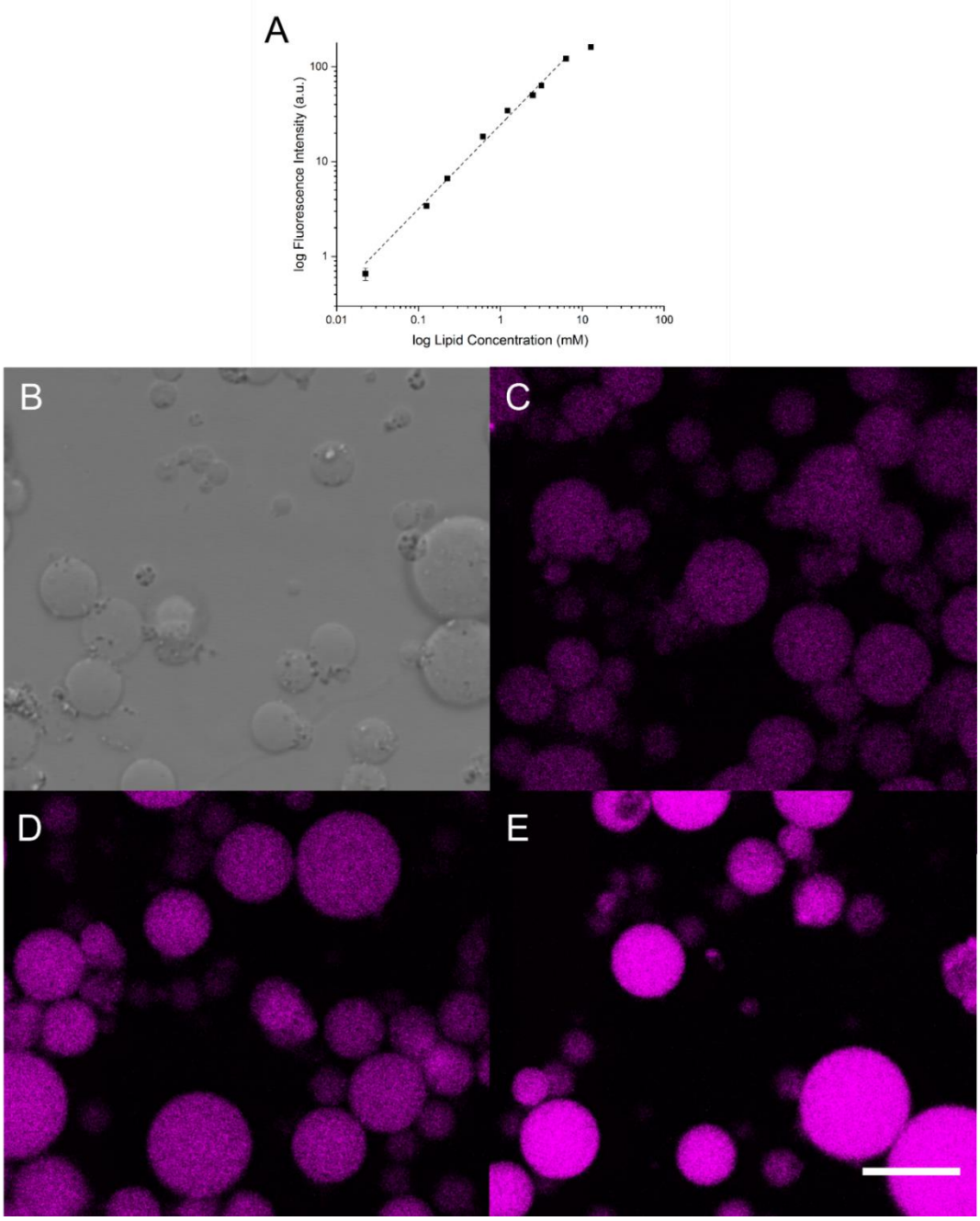

Fig. S5. Quantifying LUV encapsulation efficiency within GUVs through confocal fluorescence microscopy. A. Log-log plot of fluorescence against total lipid concentration of 1:1 DOPC:DOPG + 1mol% Rhodamine-PE large unilamellar vesicles. n=9, error bars = 1 S.D. Linear fit applied (excluding 12.7 mM value due to lack of linearity) using OriginPro 9. m = 0.886 ± 0.032, c = 1.388 ± 0.019, r^2 = 0.992. **B.** Example bright-field image of POPC nested vesicles containing 1:1 PC:PG+1mol% Rh-PE. **C/D/E.** Example fluorescence microscopy images of POPC nested vesicles containing Rh-PE labelled-LUVs at a starting concentration of 3.175, 6.35 and 12.7 mM total lipid concentration respectively. Scale bar for each image = 20 µm.

Table S2. Encapsulation Efficiency (E.E.) of PC:PG vesicles in nested vesicles

Initial Lipid Concentration (mM)	Encapsulated Lipid Concentration (mM)	Experimental E. E. (%)
6.35	4.38 ± 0.08	68.96 ± 2.63
3.175	2.11 ± 0.03	66.21 ± 2.02

N = 200, error bars = 1 S.D. for initial concentration calculation, propagation of error for E. E. estimation.

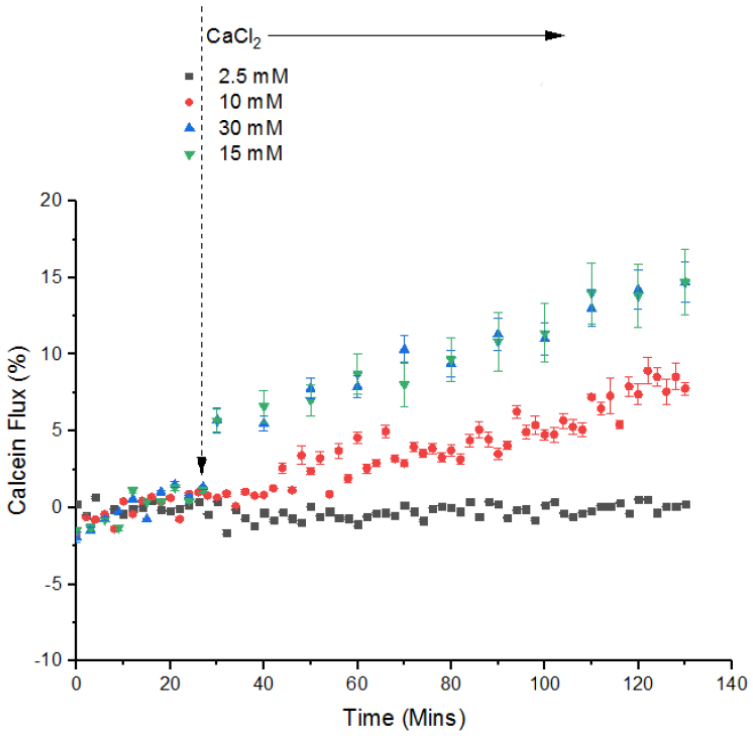

Fig. S6. Kinetics profiles of nested vesicles containing the mechanosensitive signaling pathway. MscL is present in the inner membranes, whilst αHL is added at 0 minutes. Increasing amounts of Ca^{2+} added to solution (2.5 – 30 mM) at 25 minutes (arrow). Data has been normalized to fluorescence readings obtained after the addition of αHL at t=0. Error bars show propagating error (n=3).

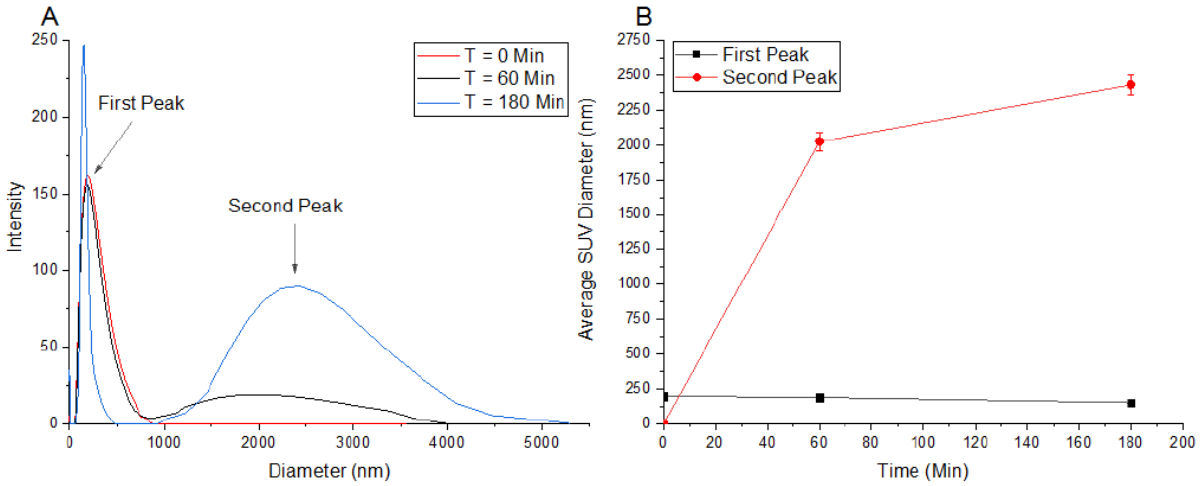

Fig. S7. Dynamic light scattering of 1:1 DOPC:DOPG vesicles in the presence of 30 mM $CaCl_2$. A. Dynamic light scattering of vesicles over three hours. At t = 0 minutes, only a single peak can be observed in solution representing extruded vesicles. A second peak begins to appear at t = 60 minutes, which increases in intensity after 3 hours, indicating that vesicle aggregation is occurring in solution. **B.** Estimation of average vesicle diameter based on peak maxima from A. over time.

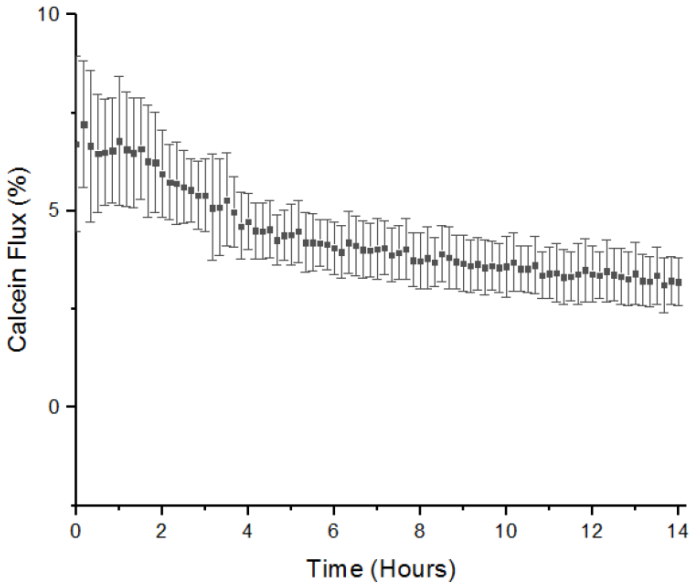

Fig. S8. Measuring the stability of nested mechanosensitive vesicles using fluorescence spectroscopy. System stability over 14 hours is confirmed by the gradual decrease in calcein fluorescence over this period. This decrease is attributed to gradual photobleaching of the calcein over time. Errors bars show 1 s.d. (n=3).

Supplementary Note 2. Comparison of Calcein Release Rates from free and nested mechanosensitive vesicles.

A single phase exponential decay function (y =A1*exp(-x/t1) +y0) was fit to the nested vesicle data from figure 1E (+MscL,+αHL) as well as from unencapsulated vesicles from figure 2A (0.5 nM $sPLA_2$ added to vesicles containing MscL to mimic $sPLA_2$ concentration found in the nested vesicles) using OriginPro 9, where y0 = offset, A = amplitude and t = time constant. Successful convergence was obtained for both fits (adj. r^2_{nested} = 0.981 and adj. r^2_{free} = 0.998 respectively). As the time constant for both fits is within error, ($t1_{nested}$ =19.61±1.36 min, $t1_{free}$=18.83±0.58 min, ±= 1 S.E.) we conclude that the rate of calcein release for mechanosensitive vesicles encapsulated in the nested system is within error of the release rate from unencapsulated vesicles, and hence compartmentalisation of the vesicles has not affected the function of the $sPLA_2$-membrane-MscL interaction.

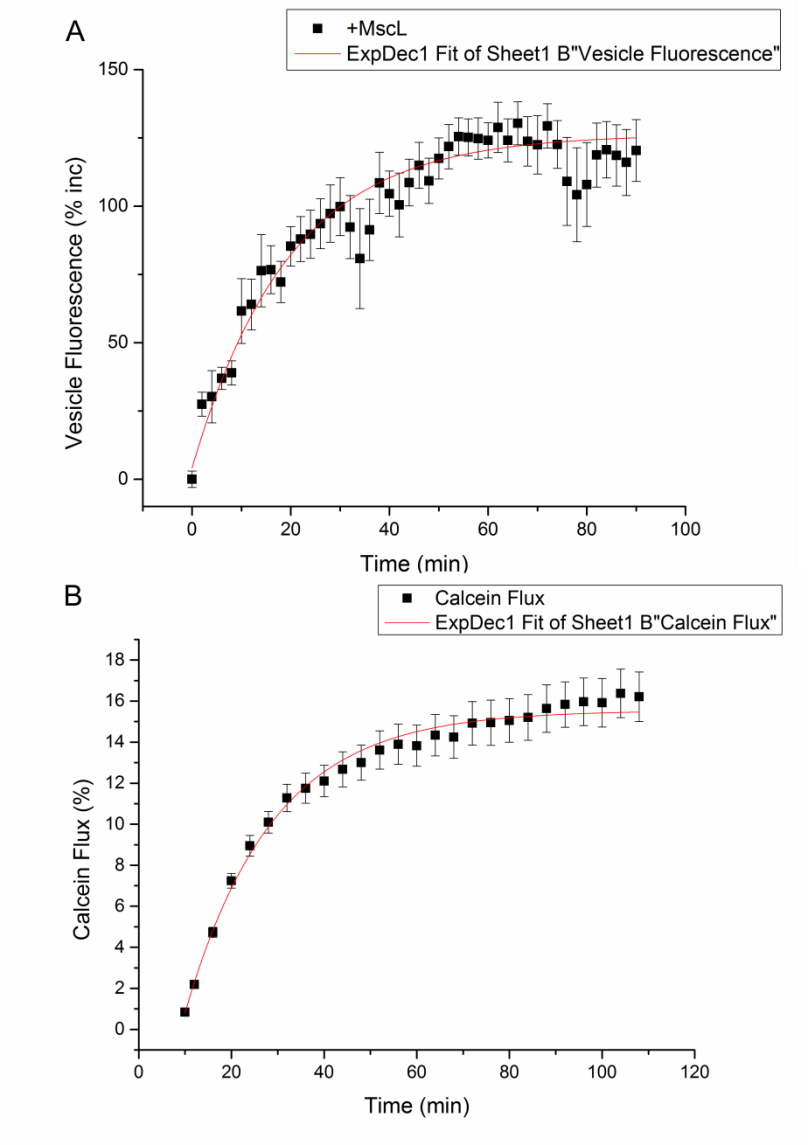

Fig. S9. Applying exponential decay (increasing form) fits to compare calcein release rate from encapsulated and unencapsulated mechanosensitive vesicles. A. Nested vesicle fluorescence (full system activation, +MscL and +αHL) and respective exponential fit (adj. r^2 = 0.981). **B.** Calcein flux from unencapsulated mechanosensitive vesicles in the presence of 0.5 nM $sPLA_2$ and respective exponential fit (adj. r^2 = 0.998).

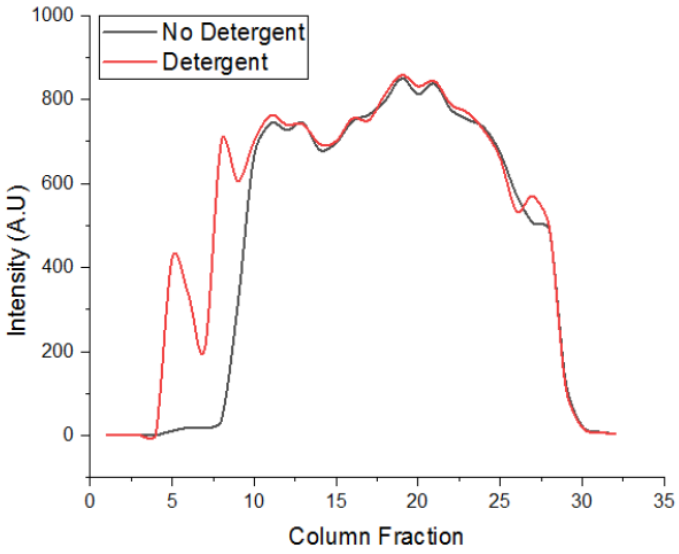

Fig. S10. Fluorescence spectroscopy of size-exclusion chromatography fractions. 32 fractions of 300 µl taken and analysed via fluorescence spectroscopy of calcein. Vesicle fractions can be observed starting from fraction 4 and finishing around fraction 8, as significant changes in calcein fluorescence can be observed upon addition of triton X-100 to these fractions. This change indicates that lysis of vesicles is occuring, liberating calcein and resulting in a fluorescence increase. Addition of Triton to later fractions results in no fluorescence change, indicating that this is unencapsulated calcein unaffected by the detergent.

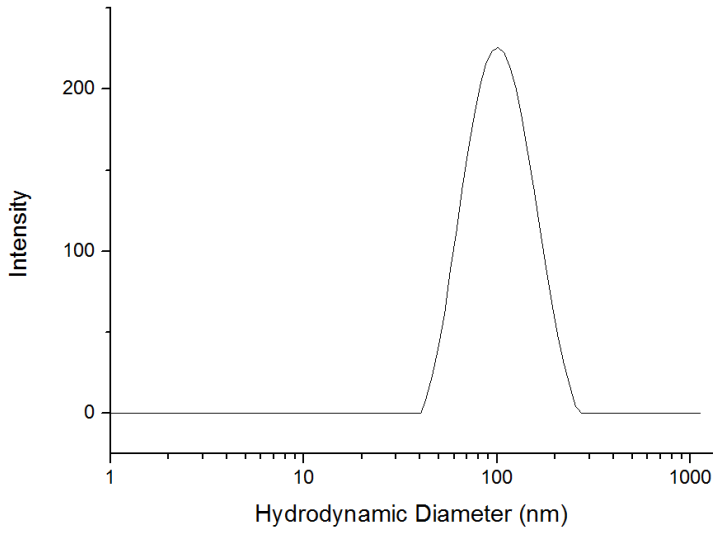

Fig. S11. Dynamic light scattering of purified calcein-loaded MscL-vesicles. Vesicles were diluted in sucrose buffer (0.5M sucrose, 20 mM HEPES, 100 mM KCl pH 7.4) at a 1:10 ratio (1 mg/ml lipid concentration) and measured at room temperature.

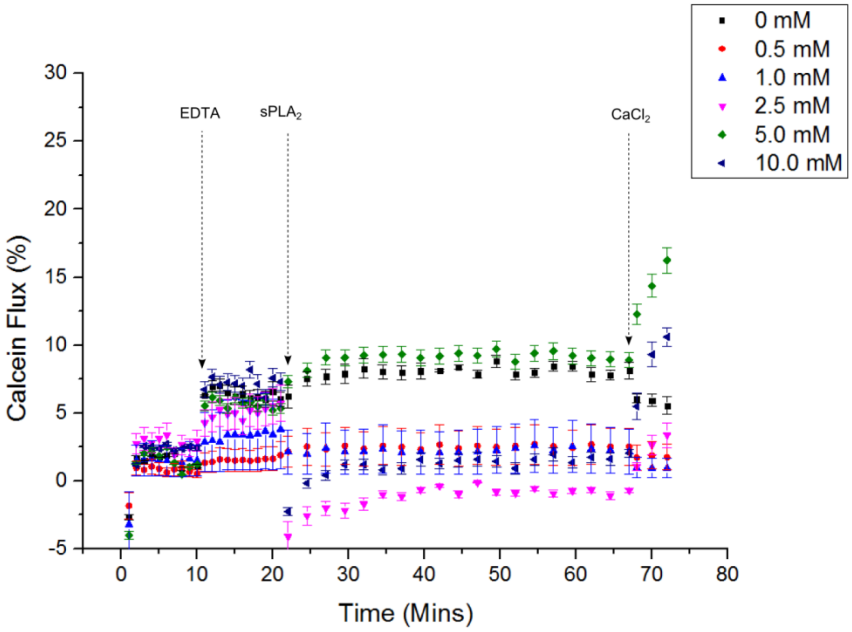

Fig. S12. Inhibition of the mechanosensitive network due to calcium chelation. Reagent addition to the well-plate resulted in small shifts in fluorescence emission due to the formation of bubbles upon mixing. This can be visualised at t= 10 minutes upon the addition of EDTA, as well as ~ t = 20 minutes after $sPLA_2$ addition, which results in a random fluorescence baseline shift. Negligible change in fluorescence occuring after this shift for 45 minutes indicates that the vesicles are stable, and this is an artefact generated through reagent addition. Due to these baseline changes calcein flux data in figure 3B. is normalised against t = 63 minutes, at which point increasing concentrations of $CaCl_2$ (0-10 mM) is added to solution re-activating the $sPLA_2$-M-MscL network. Error bars show propagating error (n=3).

References

1. Perozo E, Kloda A, Cortes DM, Martinac B (2001) Site-directed Spin-labeling Analysis of Reconstituted Mscl in the Closed State. *J Gen Physiol* 118(August):193–205.
2. Powl AM, East JM, Lee AG (2008) Anionic phospholipids affect the rate and extent of flux through the mechanosensitive channel of large conductance MscL. *Biochemistry* 47(14):4317–4328.
3. Charalambous K, et al. (2012) Engineering de novo membrane-mediated protein-protein communication networks. *J Am Chem Soc* 134(13):5746–5749.
4. Hindley JW, et al. (2018) Light-triggered enzymatic reactions in nested vesicle reactors. *Nat Commun* 9(1):1093.
5. Yoshimura K, Batiza a, Kung C (2001) Chemically charging the pore constriction opens the mechanosensitive channel MscL. *Biophys J* 80(5):2198–2206.
6. Melcrová A, et al. (2016) The complex nature of calcium cation interactions with phospholipid bilayers. *Sci Rep* 6(1):38035.
7. St. Croix CM, Shand SH, Watkins SC (2005) Confocal microscopy: comparisons, applications, and problems. *Biotechniques* 39(6S):S2–S5.
8. Venkatesan GA, et al. (2015) Adsorption Kinetics Dictate Monolayer Self-Assembly for Both Lipid-In and Lipid-Out Approaches to Droplet Interface Bilayer Formation. *Langmuir* 31(47):12883–12893.
9. Kisak E, Coldren B, Evans C, Boyer C, Zasadzinski JA (2004) The Vesosome - A Multicompartment Drug Delivery Vehicle. *Curr Med Chem* 11(2):1241–1253.
10. Boyer C, Zasadzinski JA. (2007) Multiple lipid compartments slow vesicle contents release in lipases and serum. *ACS Nano* 1(3):176–182.
11. Zhang X, et al. (2019) Multicompartmentalized vesosomes containing DOX loaded liposomes and 5FU loaded liposomes for synergistic tumor treatment. *New J Chem* 43:4895.
12. Walker SA, Kennedy MT, Zasadzinski JA (1997) Encapsulation of bilayer vesicles by self-assembly. *Nature* 387(6628):61–64.